Title: Elevated CO_2 improved the growth of a double nitrate reductase defective mutant of Arabidopsis thaliana: the importance of maintaining a high energy status

Authors: Ivan Jauregui, Pedro M[a] Aparicio-Tejo, Edurne Baroja, Concepción Avila, Iker Aranjuelo

PII: S0098-8472(17)30136-3
DOI: http://dx.doi.org/doi:10.1016/j.envexpbot.2017.06.003
Reference: EEB 3245

To appear in: *Environmental and Experimental Botany*

Received date: 15-2-2017
Revised date: 2-6-2017
Accepted date: 8-6-2017

Please cite this article as: Jauregui, Ivan, Aparicio-Tejo, Pedro M[a], Baroja, Edurne, Avila, Concepción, Aranjuelo, Iker, Elevated CO2 improved the growth of a double nitrate reductase defective mutant of Arabidopsis thaliana: the importance of maintaining a high energy status.Environmental and Experimental Botany http://dx.doi.org/10.1016/j.envexpbot.2017.06.003

Elevated CO_2 improved the growth of a double nitrate reductase defective mutant of Arabidopsis thaliana: the importance of maintaining a high energy status

Ivan Jauregui[1,2*#], Pedro Mª Aparicio-Tejo[1], Edurne Baroja [2], Concepción Avila[3], Iker Aranjuelo [2]

[1] Dpto. Ciencias del Medio Natural, Universidad Pública de Navarra, Campus de Arrosadía, E-31192-Mutilva Baja, Spain.

[2] Instituto de Agrobiotecnología (IdAB), Universidad Pública de Navarra-CSIC-Gobierno de Navarra, Campus de Arrosadía, E-31192-Mutilva Baja, Spain.

[3] Biología Molecular y Bioquímica, Instituto Andaluz de Biotencología, Unidad Asociada UMA-CSIC, Universidad de Málaga, Campus Universitario de Teatinos, E-29071 Málaga, Spain

[#] Present address: Lancaster Environment Centre, Lancaster University, Lancaster, LA1 4YQ, United Kingdom

Running title: high energy status overcomes ammonium toxicity under elevated [CO_2]

Number of tables: 2

Number of figures: 5

Supplemental data: 18

Key words: [CO_2], plant physiology, nitrate reductase, ammonium, photosynthesis, root-to-shoot, transcriptomics, redox

Corresponding author:

Name: Ivan Jauregui

Address: Lancaster Environment Centre, Lancaster University, Lancaster, United Kingdom. LA1-4YQ.

E-mail address: i.jauregui@lancaster.ac.uk

Highlights:

- Elevated [CO_2] improved the growth of the nitrate reductase double mutant, showing comparable leaf biomass accumulation as wild type plants.
- We identify as key factors explaining this response the high energy status and the adequate ROS balance of this mutant under elevated [CO_2].
- The reduced growth observed for the mutant under ambient [CO_2] is related to the emergence of ammonium toxicity syndrome.
- Our results highlight the relevance of the ammonium as N source under elevated CO_2 conditions.

Abstract:

Impairments in leaf nitrogen (N) assimilation in C_3 plants have been identified as processes conditioning photosynthesis under elevated [CO_2], especially when N is supplied as nitrate. Leaf N status is usually improved under ammonium nutrition and elevated [CO_2]. However, ammonium fertilization is usually accompanied by the appearance of oxidative stress symptoms, which constrains plant development. To understand how the limitations of direct fertilization with ammonium (growth reduction attributed to ammonium toxicity) can be overcome, the effects of elevated [CO_2] (800 ppm) exposure were studied in the *Arabidopsis thaliana* double nitrate reductase defective mutant, *nia1-1/chl3-5* (which preferentially assimilates ammonium as its nitrogen source). Analysis of the physiology, metabolites and gene expression was carried out in roots and shoot organs. Our study clearly showed that elevated [CO_2] improved the inhibited phenotype of the nitrate reductase double mutant. Both the photosynthetic rates and the leaf N content of the NR mutant under elevated CO_2 were similar to wild type plants. The growth of the nitrate reductase mutant was linked to its ability to overcome ammonium-associated photoinhibition processes at 800 ppm [CO_2]. More specifically: (i) the capacity of NR mutants to equilibrate energy availability, as reflected by the electron transport equilibrium reached (photosynthesis, photorespiration and respiration), (ii) as well as by the upregulation of genes involved in stress tolerance were identified as the processes involved in the improved performance of NR mutants.

Introduction

Although the response of plants under elevated [CO_2] is highly variable, several studies have highlighted the reduction in leaf N concentration (Loladze, 2014) as a factor that conditions photosynthetic rates. The overall leaf N status under elevated [CO_2] has been associated with decreases in photosynthetic enzymes such as Rubisco (Ainsworth and Long, 2005) and reductions in total protein concentration (Taub et al. 2008), which have generally led to decreases in photosynthetic rates. Bloom et al. (2010; 2002) have proposed that elevated [CO_2] directly affects N status in C_3 plants because of the close relationship between photorespiration and leaf nitrate (NO_3^-) assimilation. Guo et al. (2013) found that ammonium assimilation increased due to the increased N demand in N-fixing plants. It was predicted that N assimilation would also be impaired under elevated [CO_2] because photorespiration is diminished by enhanced [CO_2] and consequently ATP synthesis is decreased (Foyer et al., 2012). Furthermore, during the night period, NO_3^- assimilation is also reduced in plants exposed to elevated [CO_2] (Rubio-Asensio et al., 2015). Such an effect would be especially important in cases where plants are exclusively fertilized with NO_3^-.

Leaf N concentration declines under NO_3^-nutrition (Carlisle et al., 2012; Jauregui et al. 2015a; Jauregui et al. 2016). Nevertheless, when N is provided to the plants in the form of ammonium nitrate (NH_4NO_3), the overall N assimilation is not affected by elevated [CO_2] (Markelz et al., 2013; Jauregui et al., 2015b). However, when ammonium is supplied as the sole N source, "ammonium toxicity" arises in many plant species (Britto and Kronzucker 2002). Multiple hypotheses have been proposed to explain ammonium toxicity syndrome: cations and root pH disturbance (Britto and Kronzucker, 2002), intercellular pH disruption (Britto et al., 2001), uncoupling of phosphorylation (Gerendás et al., 1997), the futile transmembrane NH_4^+ cycling hypothesis (Britto et al., 2001), or a lack of enough C skeletons

for ammonium assimilation (Britto and Kronzucker, 2005). Nevertheless, detecting the primary mechanism of ammonium toxicity is very challenging.

Designing appropriate experiments to analyze the impact of NH_4-based nutrition on plant responsiveness to elevated [CO_2] is a matter of great importance and complexity. As shown in Supplemental Figures 1-3, in previous studies we attested that *Arabidopsis thaliana* plants grown with ammonium as the sole N source were unable to develop in our growth conditions –inhibited phenotype- despite regular pH adjustment of the solution to 5.8 (corresponding to the pH of Murashige and Skoog (MS) medium), buffered with $CaCO_3$ and replaced regularly. Within this context, to test the impact of NH_4-based nutrition in plant responsiveness to elevated [CO_2] we conducted the current study with a double nitrate reductase defective mutant (*nia1-1/chl3-5*; Wilkinson and Crawford, 1993) exposed to elevated [CO_2] (400 *versus* 800 ppm). This mutant mainly uses ammonium as the N source because it has substantially reduced nitrate reductase activity, down to 1 % in the leaves and undetectable in the roots (Wang et al., 2004). Although the inhibition of NR activity of the mutant under elevated CO_2 and nitrate nutrition has been previously described (Du et al., 2016) it is unclear whether elevated CO_2 can alleviate ammonium stress. Our working hypothesis is that an increase in C availability promotes ammonium nutrition due to more efficient management of energy and that the biomass and photosynthetic rates of NR mutant plants will be enhanced under elevated [CO_2] conditions. Physiological parameters such as photosynthetic activity, the metabolite profile (carbohydrate and amino acids), total soluble protein and N concentrations, anion and cation concentrations, and the gene expression using microarrays have been determined in shoot and root tissues.

Materials and methods:

Plant material and experimental design

The experiments were conducted in hydroponic culture with *Arabidopsis thaliana* plants, Columbia 0 ecotype (wild type) and the Columbia 0 ecotype double nitrate reductase defective mutant *nia1-1/chl3-5* (NR mutant). Seeds were germinated in an agar matrix using a seed holder system (Araponics, Liège, Belgium). Germination took place in a growth chamber that maintained dark conditions for 48h at 24ºC, with distilled water providing moisture and saturated humidity. Plants were transferred to a growth chamber for 13 days at 150 μmol m^{-2} s^{-1} PAR with a short day photoperiod (8/16 h day/night), a 22-18 ºC (day/night) thermoperiod, under saturated humidity and with atmospheric [CO_2] concentration (400 ppm [CO_2]). Subsequently, Arabidopsis plants of uniform size were selected and transferred to hydroponic containers 15 days after sowing (2 days germination and 13 days in a growth chamber). The capacity of the hydroponic containers was 8 liters, and each container had 12 plants (6 wild type and 6 NR mutant plants). Plants were cultured in two different controlled-environment chambers (Heraeus-Votsch HPS-500, Norrkoping, Sweden) of 500 L capacity at two different [CO_2] levels: 400 ppm (atmospheric [CO_2]) and 800 ppm (elevated [CO_2]) for 4 weeks (28 days). The growth chamber conditions were kept at 22/18 ºC (day/night), a short day photoperiod (8/16 h day/night), 80% rH and 200 μmol $m^{-2}s^{-1}$ PAR. In order to confirm the physiological response, the experiment was replicated. The plants were rotated between the chambers in order to avoid chamber effect phenomena. In total, the experiment was conducted with 24 replicates per treatment across two experiments for the growth parameters and 3-6 replicates for other measurements. The gene expression analysis was conducted using plants from only one of these pseudoreplicates, as has been done in previous publications (Leakey et al., 2009). Two containers (12 plants per container, 6 for each ecotype) per [CO_2] treatment were used in each experiment. N-free modified Rigaud and Puppo's solution

(Puppo and Rigaud, 1975) was used (1.15mM K_2HPO_4; 2.68mM KCl; 0.7mM $CaSO_4$; 0.07mM Na_2Fe–EDTA; 0.85mM $MgSO_4$; 16.5µM Na_2MoO_4; 3.7µM $FeCl_3$; 3.4µM $ZnSO_4$; 16µM H_3BO_3; 0.5µM $MnSO_4$; 0.1 µM $CuSO_4$; 0.2 µM $AlCl_3$; 0.1 µM $NiCl_2$; 0.06 µM KI) . The pH was adjusted to 5.8 with H_3PO_4 and buffered with $CaCO_3$ (0.5 mM) to avoid acidification of the solution. This pH corresponds to the pH of MS medium. The N source was NH_4NO_3 at 1 mM concentration. The solution was replaced every 3-4 days.

All determinations were conducted after 4 weeks exposure to [CO_2] treatments, before the first flower buds were visible and when the more advanced phenology treatment (elevated [CO_2]) was at the 3.7 growth stage of ontology using the scale of Boyes (2001).

Plant growth determinations and gas exchange

Plant sampling was always carried out 5 h after the beginning of the illumination period. The shoot tissue was harvested and immediately frozen in liquid nitrogen and stored at -80ºC for further analysis. After that, the root tissue was cleaned with abundant MilliQ water, dried with paper, frozen in liquid nitrogen and stored at -80ºC. For plant growth determinations, samples were dried at 70°C for 48 h to obtain the dry biomass (DM).

Gas exchange measurements were carried out with a Li-COR 6400XT portable gas exchange system (Li-COR, Lincoln, Nebraska, USA) on fully expanded leaves. Such measurements were conducted between 4 h and 7 h after the onset of the light period. The net photosynthetic rates (A_n) were measured at 200 µmol m^{-2} s^{-1} Photosynthetic Photon Flux Density (PPFD). The light-saturated rate of [CO_2] assimilation was measured under saturated light conditions (1000 µmol m^{-2} s^{-1} PPFD) in order to estimate the maximum carboxylation velocity of Rubisco (Vc_{max}) and the maximum electron transport rate contributing to RuBP regeneration

(J_{max}) using the model of Harley et al. (1992). The equipment conditions during the measurements were: air flow rate 400 µmol s^{-1}; block and leaf temperature 25°C; relative humidity in the sample cell 60%. We selected 9 points (7 [CO_2] levels) for these model curves (400, 250, 100, 250, 400, 600, 800, 1000 and 1200 µmol mol^{-1} [CO_2]). The dark respiration (R_d) measurement was performed 30 min after the dark period started; measurements were made in automatic mode and therefore leaves were placed in the chamber for at least 10 min. The transpiration rate (E) and intercellular [CO_2] (C_i) and were obtained with a Li-COR 6400XT portable photosynthesis system. The relative quantum efficiency of PSII photochemistry (Φ_{PSII}) and the electron transport rate (ETR) were measured simultaneously with a fluorescence chamber (LFC 6400-40; Li-COR) coupled to the Li-COR 6400XT. The rate of electron transport through PSII [Je(PSII)], the electron flux for photosynthetic carbon reduction [J*e*(PCR)] and the electron flux for photorespiratory carbon oxidation [J*e*(PCO)] were measured as described by Epron et al. (1995).

Metabolite determinations

Soluble sugar and starch determination

Frozen plant material (0.1 g) was ground using liquid nitrogen and then collected in a plastic vial with 1 ml of 80% ethanol. The sample was sonicated for 25 min at 30ºC using an ultrasonic bath (Selecta, Barcelona, Spain) and centrifuged at 16000 g to collect the supernatant. The same procedure was repeated 3 times. The supernatant was evaporated through a TurboVap (Carmel, New York, USA). After evaporation, the sample was re-suspended in 1.5 ml of H_2O via a vortex step and in an ultrasonic bath. Finally, the extract was centrifuged and the aqueous fraction selected. The solid phase was dried at 70ºC for 24 h to measure starch content. Soluble sugars (sucrose, glucose, and fructose) were determined from the aqueous fraction and starch content from the dry pellet using capillary

electrophoresis (Beckman Instruments, Fullerton, California, USA) as detailed in Jauregui et al. (2016). Fucose was used as the internal standard and was added to the extract to be tested (0.5 mM final concentration of fucose).

Starch content was determined in the dry pellet obtained as detailed in the extraction procedure above. The pellet was resuspended in the plastic tube with milli-Q water using a vortex. The total material was homogenized with an ultrasonic bath for 10 min and then incubated for 1 h at 100°C. Then the extract was cooled to room temperature. To hydrolyze all the starch present in the sample, 30% vol/vol of amyloglucosidase solution was added (41 mg of previously desalted amyloglucosidase enzyme in 50 ml of NaAc buffer, 8.55 mM, pH 4.5). Amyloglucosidase was desalted on Bio-Rad Bio-Gel P-6-DG acrylamide gel columns with the following desalting buffer: 250 mM MOPS, 25 mM $MgCl_2$, 100 mM KCl, pH 7. The extracts were homogenized with a vortex after the addition of amyloglucosidase solution and incubated at 50°C for about 12 h. After that, the extracts were centrifuged at 4800 g and the supernatant recovered and stored at -20°C until quantification of the glucose in the samples by capillary electrophoresis as detailed in Jauregui et al. (2016).

Amino acid content determinations

Frozen plant tissue (0.1g) was ground with liquid nitrogen, homogenized with 1 ml of 1M HCl and then transferred to a plastic vial. The extract was incubated for 10 min on ice and centrifuged at 16000g and 4ºC for 10 min. The supernatant was neutralized with NaOH and stored at -20ºC. Amino acids were derivatized at room temperature for between 12-16 h with FITC dissolved in 20 mM acetone/borate, pH 10. Single amino acids were determined by high-performance capillary electrophoresis using a Beckman Coulter PA-800 apparatus (Beckman Coulter Inc., California, USA) according to Jauregui et al. (2016). The internal

standard, norvaline, was used. The protocol did not allow separate analyses of glycine and serine, so they were quantified together.

Protein determinations

Total soluble protein

Frozen plant tissue (0.1 g) was ground with liquid nitrogen and homogenized with the following buffer: 50 mM Tris-HCl (pH 8), 1 mM EDTA, 10 mM 2-mercaptoethanol, 5 mM DTT, 10 mM $MgSO_4$, 1 mM cysteine, 0.5 % PVPP, and 1mM PMSF. The extract was transferred to a plastic vial and centrifuged at 16000 g at 4ºC for 10 min. Then the supernatant was collected. Total soluble protein was quantified using the Bradford micro-assay (Bradford, 1976).

Enzyme assays

All enzymatic reactions were carried out at 37°C. Frozen plant tissue (100 mg) structures were homogenized with mortar and was resuspended at 4°C in 5 ml of 100 mM HEPES (pH 7.5), 2 mM EDTA, and 5 mM dithiothreitol. The suspension was desalted and assayed for enzymatic activities. GS was assayed as described by Baroja- Fernández and col., (2009). NR was assayed following the method of González et al., (2001). One unit (U) is defined as the amount of enzyme that catalyzes the production of 1 μmol of product per minute.

Western blot analyses

For SDS-PAGE, 25 μl of total soluble protein was mixed and denatured with the following loading buffer (62 mM Tris-HCl (pH 6.8), 50% glycerol, 5% 2-mercaptoethanol, 2.3% SDS and 0.1% blue bromophenol) and was boiled at 100ºC for 5 min. Samples were added to acrylamide gels (12.5% m/v) and run at 125 V for 1 hour with running buffer (25mM Tris,

192 mM glycine, 0.1 mM SDS). SDS–PAGE was performed with an anti-GS IgG antibody (Cruz et al., 2011). The dilution used was 1:2000. A peroxidase conjugated goat anti-rabbit IgG, followed by luminescence detection with the ECLTM Plus kit (Amersham Biosciences, Buckinghamshire, UK), was used.

Elementary analysis

Nitrogen and carbon concentrations

Leaf N and C content were determined in the dry material using a CNS 2500 elemental analyzer (CE Instruments, Milan, Italy). The C/N ratio was calculated from N and C percentage data.

Nitrate and cation concentrations

Nitrate and cation (ammonium, magnesium, potassium and calcium) concentrations were determined in the aqueous fraction of the metabolite analysis described above with an isocratic ion chromatography technique using a DIONEX-DX500 system (Dionex Corporation, California, USA). For anion concentrations, an IonPac AS11 column connected to an ATC-1 protecting column and an AG11 pro-column were used (all equipment obtained from Dionex, Salt Lake City, USA). For cation concentrations, IonPac CG12A and CS12A columns were used.

Gene expression

RNA isolation and microarray analysis

Three biological replicates were used for each treatment and tissue. RNA was isolated as described by Liao et al. (2004). RNA concentration and purity was determined spectrophotometrically (NanoDrop ND-1000A UV-Vis spectrophotometer, Wilmington, USA) as detailed by Jauregui et al. (2015b).

To identify differences in gene expression an Agilent 4x44 K Arabidopsis microarray with single color (Cy_3) labeling was used. The microarray slides were hybridized, stained and washed as recommended by the manufacturer's protocol (Agilent Technology, California, USA). Hybridized slides were scanned using a GENEPix 4100A Microarray Scanner (Molecular Devices, California, USA).

The microarray data have been deposited in NCBI's Gene Expression Omnibus (Edgar et al., 2002) and are accessible through GEO Series accession number GSE64994: http://www.ncbi.nlm.nih.gov/geo/query/acc.cgi?acc=GSE70560

The gene classifications for the functional categories are based on MapMan (Thimm et al., 2004; http:// gabi.rzpd.de/projects/MapMan/ v. 1.5.0).

qPCR validation

Real-time quantitative PCR was used to validate selected genes from the microarray experiments with experimental gene profiles in the same samples as detailed by Jauregui et al. (2015b). The genes selected varied across the whole range of fold changes observed in the microarray results (Supplemental Tables 1). Gene-specific primer sequences for amplification are described in Supplemental Table 2 and the results can be seen in Supplemental Figure 1.

Statistical analysis

Statistical analysis for all measurements analyzed, with the exception of microarray analysis, was performed by one factor ANOVA (SPSS v.12.0; Chicago, USA). The results were accepted as significant with $P \leq 0.05$.

Three replicates per treatment and tissue were conducted for the microarray analysis. Background correction was performed with the quantile between arrays method as described by Bolstad et al. (2003). A linear model was fitted with limma (Smyth, 2004) and corrected by adjusting *P* values using the Benjamini and Hochberg method (1995). Leaf and root tissues were compared separately. For this study, a significant difference in gene expression was determined at a *Q value* ≤ 0.05 and $\log_2$ fold change ≥ 0.5.

Results:

Plant growth

Our study revealed that, regardless of the analyzed genotype (wild type or NR mutant), exposure to elevated [CO_2] increased shoot, root, and total biomass (Figure 1). More specifically, the biomass increases found for wild type plants were 350% in shoots and 460% in root tissues (Figure 1 A-B). In NR mutant plants, elevated [CO_2] increased shoot and root biomass by a notable 970% and 1620%, respectively (Figure 1 A´-B´, Suppleental Figure 5). When we compared both genotypes (wild type *versus* NR mutant plants) there was a significant decrease in growth of the NR mutant at 400 ppm [CO_2]: a 68% reduction in shoots and 81% in roots compared to wild type plants. Nevertheless, no differences in biomass were found in leaves under elevated [CO_2] conditions between wild type and NR mutant plants. The root tissue was reduced 27%.

Leaf gas exchange measurements

The photosynthetic rate (An) was enhanced by up to 150% in wild type plants exposed to 800 ppm and 420% in NR mutant plants. The maximum rate of Rubisco carboxylase activity (Vcmax) showed an increase of 30% in the wild type and 130% in the NR mutant (Figure 2 B-B´). Likewise, the maximum electron transport rate contributing to RuBP regeneration (Jmax) showed similar increases in plants exposed to elevated [CO_2]: 30% for wild type and 175% for NR mutant plants (Figure 2 C-C´). The An of the NR mutant at 400 ppm was lower than wild type plants under the same conditions (45%), as were Vcmax (40%) and Jmax (52%). Interestingly, this trend was not repeated under elevated [CO_2]: no differences in An, Vcmax or Jmax between wild type and NR mutant plants were observed. Besides, leaf intercellular [CO_2] (Ci) was approximately twice the ambient level, at nearly 800 ppm under elevated [CO_2], in both genotypes (Figure 2 E-E´). The leaf dark respiration rates (Rd) were

higher in plants exposed to elevated [CO_2] (Figure 2 D-D´). When compared to the NR mutant with wild type grown in same conditions we found a reduction in the dark respiration: 80% in ambient [CO_2] concentrations and 20% at elevated [CO_2].

Regardless of the genotype, the electron transport rate (Je(PSII)) increased in plants exposed to elevated [CO_2]: 60% in wild type plants and up to 200% in NR mutants (Figure 4 A-A´). These differences were not found when we compared the genotypes under elevated [CO_2] conditions; nevertheless, Je(PSII) noticeably diminished (by 50%) in the NR mutant in comparison to wild type plants under ambient [CO_2] conditions (Figure 3 A-A´). Similar patterns were detected for electron flux for photosynthetic carbon reduction [Je(PCR)] and electron flux for photorespiratory carbon oxidation [Je(PCO)]. The exposure to elevated [CO_2] increased both parameters regardless of the genotype, and it was appreciably reduced in NR mutant plants under ambient [CO_2]. Therefore, the Je(PCR) /Je(PCO) ratio revealed that under elevated [CO_2], carboxylation is promoted over oxygenation. At the same time, we observed a slight decrease in the Je(PCR) /Je(PCO) ratio in NR mutant plants under ambient [CO_2], whereas no significant differences were detected under elevated [CO_2]. In wild type plants grown under elevated [CO_2] a 30% increase in the relative quantum yield of PSII at the steady state (ΦPSII) was detected. However, between both genotypes no significant changes in ΦPSII were observed under elevated [CO_2] conditions. NR mutant plants exposed to elevated [CO_2] had a 150% increase in ΦPSII when compared to plants exposed to atmospheric concentrations.

Plant nitrogen status, total soluble protein, NR and GS activity, GS amount

Leaf N status was not altered by elevated [CO_2] in wild type plants (Table 1). Nevertheless, the leaf N concentration was reduced in NR mutant plants exposed to elevated [CO_2]. We

found that leaf N concentration was not modified under elevated [CO_2] when comparing NR mutant and wild type plants. However, we found a 10% increase in N concentration in leaves of NR mutant plants compared to wild type plants grown under ambient [CO_2]. Thus, the C/N ratio was reduced by 20% in NR mutant plants grown under ambient [CO_2], whereas it was not modified in wild type plants. Leaf total soluble protein (TSP) was reduced in plants under elevated [CO_2] in both genotypes, but was more significant in NR mutant plants. Hence, NR mutant plants grown under ambient [CO_2] showed a 30% increase in TSP compared to wild type plants grown under the same conditions (Table 1). Nevertheless, no differences were found when both Arabidopsis genotypes were grown under elevated [CO_2] conditions. It is noteworthy that NR mutant plants under elevated CO_2 did not suffer N limitation (Table 1), despite NR activity was 96% lower in leaf and not detectable in root (Supplemental Figure 6). The NR activity of this plants under ambient CO_2 was lower than 98% of wild type plants in ambient CO_2. We do not found differences on NR activity comparing the genotype performance under ambient and elevated [CO_2]. Root NR activity were not found in NR mutant plants (Supplemental Figure 6), and not differences where found in the wild type plants. The leaf GS activity was a slightly lower in NR mutant plants under ambient CO_2 and we found an increments 12% in GS activity comparing to wilt plants in this conditions and a 7% more activity comparing to NR mutants under elevated CO_2. We found a reduction of root GS activity in the NR mutant plants, although no differences were found between the CO_2 treatments. Finally, no differences in leaf GS content (Supplemental Figure 8) were found.

Nitrate, ammonium and cations

Leaf nitrate (NO_3^-) concentration was reduced under elevated [CO_2] in both genotypes: wild type showed a 30% and NR mutant a 17% reduction of [NO_3^-] comparing to the genotype

grown under ambient [CO_2] (Table 1). Further, NR mutant plants showed higher [NO_3^-] than wild type plants in both CO_2 treatments. At the same time, root [NO_3^-] was higher (10%) in NR mutant plants grown under ambient [CO_2] compared to wild type plants grown under the same conditions. The leaf ammonium concentration was higher in both genotypes in plants grown under ambient [CO_2] (Table 1). Likewise, we found a huge increase of 300% in leaf ammonium concentration in NR mutant plants grown under ambient [CO_2] conditions compared to wild type plants under the same conditions. The root ammonium concentration was higher in NR mutant plants under elevated [CO_2], while no differences were found in wild type plants. Finally, the analysis of the cations concentration indicated a huge reduction in NR mutant plants under ambient [CO_2] in both tissues (Supplemental Table 3). Likewise, cations concentration were modified in wild type plants exposed to 800 ppm [CO_2]: leaf magnesium (Mg^{+2}) and calcium (Ca^{+2}) were reduced under elevated CO_2 conditions. At the same time, root Mg^{+2} and Ca^{+2} were higher in roots of plants exposed to elevated CO_2. Meanwhile, NR mutant plants exposed to elevated CO_2 shown greater increases in cations in both tissues.

Metabolomics profile

The leaf carbohydrate (Figure 4 A) content was modified in wild type plants exposed to 800 ppm [CO_2]. While the sucrose, glucose, and starch content increased, no significant changes were found in fructose levels. At the root level, we found a slight decrease in starch in plants exposed to elevated [CO_2] (Figure 4 B). Meanwhile, NR mutant plants showed increases in sucrose and glucose under elevated [CO_2], but fructose levels were not modified (Figure 4 C´). Starch content was remarkably high in both [CO_2] treatments. Nevertheless, no significant differences were found. In root tissue, we found decreases in sucrose glucose and fructose in plants under elevated [CO_2].

Transcriptional profile

Gene expression was analyzed using microarrays and showed a wide range of responses associated with each factor: genotype, [CO_2] treatment, and organ. As shown in Table 2, in wild type plants exposed to elevated [CO_2], more genes were expressed differentially in roots than in shoots (212 and 856 respectively); 75 % of the total genes differently expressed in leaves were upregulated in leaves of plants exposed to 800 ppm, while this activity was not found in root tissues. A higher number of genes were differentially expressed in NR mutant plants. As shown in Table 2, 1947 genes were differentially expressed in leaves and 1379 in roots. When genes were organized by functional categories, the metabolic pathways most represented in wild type leaves under elevated [CO_2] were: signaling, protein modification, stress, cell modification and secondary metabolism. In root tissue, the genes were not classified in any preferential functional groups that stood out under the [CO_2] treatment. Meanwhile, the numerous metabolic pathways in leaves of NR mutant plants exposed to elevated [CO_2] were: transport, signaling, stress, hormone metabolism and sugar metabolism, while the photosynthesis functional group was downregulated. In root tissues of NR mutant plants, elevated [CO_2] induced the expression of genes in the following functional categories: photosynthesis, glycolysis, protein, transport, hormone metabolism, secondary metabolism, cell, electron transport and fermentation.

Discussion:

The responsiveness of Arabidopsis plants to elevated [CO_2] has been extensively studied in recent years (Rubio-Asensio and Bloom, 2016; Niu et al. 2016; Jauregui et al . 2016; Jauregui et al. 2015: Hachiya et al., 2014; Markelz et al., 2013; Niu et al. 2013; Li et al., 2008). Bloom and coworkers (2014; 2002) suggested that compared to nitrate, ammonium nutrition might favor N assimilation under elevated [CO_2] conditions. The linkages between nitrate assimilation and photorespiration have been recently described (Fan et al., 2016) using another approach: rice plants overexpressing the nitrate transporter NRT2.3b, which enhanced yield and N content, showed both reduced photorespiration and enhanced ammonium absorption. However, providing ammonium as the main N fertilization form has been described (Britto and Kronzucker, 2002) to be deleterious for plant performance and, independent of the [CO_2], biomass production is reduced under NH_4^+ nutrition compared to NO_3^- nutrition under elevated CO_2 (Carlisle et al., 2012; Rubio-Asensio et al., 2015; Niu et al., 2013; Rubio-Asensio and Bloom, 2016). Within this context, our study aims to discuss the mechanisms that allow NR mutant plants to substantially overcome the inhibited phenotype associated with elevated [CO_2].

The overall superior performance of wild type plants under elevated [CO_2].

In agreement with previous studies (Jauregui et al., 2015; 2016) the larger photosynthetic rates of wild type plants exposed to elevated [CO_2] was reflected in larger biomass production of those plants. While the gene expression analyses did not remark a significant increase in the expression of Calvin cycle proteins, the larger Ci, together with the larger *in vivo* Rubisco and RuBP regeneration activity determinations (Vcmax and Jmax respectively), explained the notorious increase in photosynthetic rates of wild type plants grown under 800

ppm. Moreover, our study also highlights the fact that higher photosynthetic rates of plants exposed to 800 ppm plants were sustained by increased energy metabolism: i.e. a superior electron transport rate (Figure 3A-D) and dark respiration rates (Figure 2D). The higher sugar content (Figure 4B) as well as genes related to sugar pathways such as glucose transport and glycolysis in root tissue in plants exposed to elevated [CO_2]. Therefore, our data suggested a more favorable C status under elevated [CO_2] throughout the whole plant. The larger carbohydrate availability contributed to increase dark respiration (Rd) activity required to match the higher energy demand of wild type plants. Similar results have been reported previously by our group (Jauregui et al. 2015b) from wild type plants grown under a long day photoperiod (16/8 h day/night). Thus, these observations suggests the existence of a conserved primary metabolism and a steward transcriptional mechanism that supported the overall superior responsiveness of Arabidopsis plants grown with mixed NH_4NO_3 nutrition and under elevated [CO_2] conditions.

NR mutant plants under ambient [CO_2] **exhibited ammonium toxicity syndrome.**

It is widely accepted that the presence of NO_3^-, even when not assimilated, can ameliorate ammonium toxicity syndrome (Hachiya et al., 2014). Nevertheless, our study highlighted the fact that the NR mutant performed differently depending on the atmospheric [CO_2]: clearly, elevated [CO_2] improved the inhibited phenotype of NR mutant plants. NR mutant plants under ambient [CO_2] exhibited an overall photosynthetic and growth suppression (Figure 1 A´-B´; Supplemental Figure 5) associated with the lower Vcmax and Jmax. In line with our results, Wang et al., (2004) reported that the inhibited growth of the NR mutant plants under NH_4NO_3 and ambient [CO_2] was higher under acidic conditions, (we used a pH of 5.8, same as MS medium). Moreover, our study remarked that the worse performance of NR mutant under ambient [CO_2] is linked with ammonium toxicity (Sarasketa et al., 2014). The first

factor related to ammonium toxicity (detected in our measurements) is the accumulation of ammonium (a huge 300% increase) in the leaves under ambient [CO_2] (Table 1), a physiological response widely described in the literature (Britto and Kronzucker, 2002). The second factor related to ammonium toxicity is the large depletion in cation concentrations in both leaves and roots (Supplemental Table 3), particularly K^+, Ca^{+2}, and Mg^{+2}, an indicative ammonium toxicity physiological response (Hachiya et al., 2014). Together, the enormous starch accumulation found in NR mutant plants under ambient CO_2 could be related to the overwhelming decrement in leaf cations described previously (Limoine et al., 2013) and where also found on Arabidopsis plants growth under ammonium nutrition (Hachiya et al., 2014). Related to this, Chen et al., (2015) proposed that the inhibited phenotype of the NR mutant is associated with the K^+ impairment phenomenon that is closely related to the above-mentioned ammonium toxicity syndrome. Taking this into account, the strong inhibition of photosynthetic machinery (Figure 2B'-C', Figure 3A') may be related to the K^+ impairment proposed by Chen et al., (2015). Thus, the physiological disturbances described support the hypothesis that NR mutants grown at ambient [CO_2] manifested symptoms associated with ammonium toxicity.

The emergence of redox imbalance.

Ammonium-based nutrition has been associated with intracellular redox imbalance (Podgórska et al., 2013; Liu and von Wirén, 2017) and impairment of the mitochondrial electron transport chain has been linked to oxidative stress under such nutritional conditions (Guo et al., 2005). As shown in Figure 3A´-D´, NR mutant plants, which mainly assimilate ammonium as the N source, showed lower Je(PSII) compared to wild type plants under ambient [CO_2] conditions (and when the NR mutant plants were exposed to elevated CO_2). Within this context, it is crucial for plants to balance their redox state. As mentioned above,

photosynthesis is a large energy demanding sink. Within this context, the fact that NR mutants showed the lowest Vcmax, Jmax (having the same Ci) revealed that photosynthetic machinery was severely impaired in those plants. As a consequence of such diminishment in photosynthesis, those plants were subjected to an over-excitation of the photosynthetic pigments in the antenna. Impairment of photosynthetic function might lead to excessive excitation energy in photosystem II (PSII) and appearance of reactive oxygen species resulting in oxidative stress (Chaves et al. 2009; Lawlor and Tezara 2009). Such idea was reinforced by the inhibition of photosystem II relative quantum yield. So the maintenance of equilibrium between light capture and photochemistry requirements is a key point for the avoidance of ROS (Niinemets and Kull 2001). The transcriptomic approach corroborates this response because genes related to the photosystem complex were highly overexpressed: 93% of the genes related to the photosystem group were upregulated in NR mutant plants under ambient [CO_2] conditions (Figure 5; Supplemental Table 1). To be noted also that redox group underlines how a vast majority of genes overexpressed under ambient [CO_2] conditions were ROS detoxifiers such as superoxide dismutases (at5g23310, at5g51100), ascorbate peroxidases (at4g09010, at4g08390), peroxiredoxins (at3g11630, at3g26060), glutathione peroxidases (at4g31870) and glutaredoxins (at5g20140, at2g20270). These results suggest that NR mutant plants under ambient [CO_2] respond to ammonium toxicity syndrome with enhancement of ROS metabolism gene expression.

Energy as a key factor conditioning the superior performance of NR mutant plants under elevated [CO_2]

In the first place, it is noteworthy that NR mutant plants in high CO_2 maintain same N status as wild type plants (Table 1): despite NR activity was 96% lower in leaf and not detectable in root (Supplemental Figure 6). The absence of differences in GS (Supplemental Figures 7-8)

nor in the accumulation of the different amino acids (Supplemental Figures 9-10) contribute to sidestep possible N limitation in the different treatments. Further, as previously described by Unkles et al. (2004), NR mutant does not show nitrate uptake impairment (Table 1). Having said this, opposite to the observations under 400 ppm [CO_2], the photosynthetic activity and plant growth of NR mutants exposed to elevated [CO_2] was similar to wild type plants grown under 800 ppm. The ability of NR mutant plants to maintain high rates of photosynthesis under elevated [CO_2] was supported by their capacity to ensure energy demand for C fixation. As shown in figure 4C´, compared to plants under ambient [CO_2] these plants showed higher sugar content alongside upregulation of genes encoding for energetic metabolic pathways (Figure 5; Supplemental Table 1). Our transcriptomic approach showed relevant information dealing with the impact of [CO_2] on photosynthetic, carbohydrate and energetic metabolism in NR mutants. First, related to the pentose phosphate pathway, the gene expression of transaldolase (at5g13420), 6-phosphogluconolactonase (at1g13700) and glucose-6-phosphate dehydrogenase (at1g24280) was powerfully correlated with enzyme activity and growth (Keurentjes et al., 2008). Second, the glycolysis pathway featured transcripts of phosphofructokinase (at4g26270, at2g22480), which performs the first committed step in the glycolytic pathway, and phosphoglucomutase (at1g70820), which controls carbon flow through starch metabolism or the tricarboxylic acid (TCA) cycle acid cycle and the pentose phosphate pathway (Periappuram et al. 2000). Finally, the tricarboxylic acid cycle may be enhanced because a number of genes were significantly increased in our experiment under elevated [CO_2] in NR mutant plants. These included: at5g50950, which encodes a fumarate hydrolase2 that has been described as promoting carbon storage and is involved in pH homeostasis (Pracharoenwattana et al., 2010); at2g05710, which encodes aconitate hydratase, a gene that is highly upregulated under elevated [CO_2] (Watanabe et al., 2014); and some TCA genes including 2-oxoglutarate dehydrogenase (at5g65750), malate

dehydrogenase (at2g19900) and citrate synthase (at2g42790). In line with the gene induction described, the NR mutant exposed to elevated [CO_2] showed greater dark respiration rates (Figure 2D´), which suggests that these plants were capable of maintaining a superior energy status under elevated [CO_2] conditions. Further, the Je(PCR) /Je(PCO) ratio revealed that under elevated [CO_2], carboxylation is promoted over oxygenation (Figure 3D').

Conclusions:

In summary, our results indicate that under elevated [CO_2], *Arabidopsis thaliana* NR mutant (*nia1-1/chl3-5* defective) plants, which are reliant on ammonium nutrition, showed a leaf development comparable to wild type plants, and were capable of using ammonium and nitrate. Indeed, the photosynthetic rates are similar between the two genotypes. We established that NR mutant plants exposed to elevated [CO_2] have substantial improvements in development due to their capacity to satisfy energy-demands for the Calvin cycle. Further, we proposed several possible mechanisms, detected at physiological and gene expression levels, which cooperate in sidestepping ammonium toxicity syndrome in NR mutant plants grown under elevated [CO_2]. Specifically, their higher C status, which ensures that the provision of ATP is linked to a reduction in photorespiration electron consumption and adequate ROS balance. Our results have shown that implementation of ammonium nutrition should enable plants to exploit the oncoming increases in atmospheric [CO_2].

Acknowledgements:

This work has been funded by the Spanish National Research and Development Programme (AGL2009-13339-C02-02, AGL2011-30386-C02-02 and AGL2012-37815-C05-05). Ivan Jauregui was the holder of a FPI fellowship from the Spanish Ministry of Economy and Competitiveness.

Bibliography:

Ainsworth, E.A., Long, S.P. 2005. What have we learned from 15 years of free-air CO_2 enrichment FACE? A meta-analytic review of the responses of photosynthesis, canopy properties and plant production to rising CO_2. New Phytol. 165, 351–371.

Aranjuelo, I., Cabrerizo, P.M., Arrese-Igor, C., Aparicio-Tejo, P.M. 2013. Pea plant responsiveness under elevated [CO_2] is conditioned by the N source (N_2 fixation versus NO3− fertilization). Environ. Exp. Bot. 95, 34–40.

Benjamini, Y., Hochberg, Y. 1995. Controlling the false discovery rate-A practical and powerful approach to multiple testing. J. R. Stat. Soc. 57, 289–300.

Bloom, A., Asensio, J., Randall, L. 2012. CO_2 enrichment inhibits shoot nitrate assimilation in C3 but not C4 plants and slows growth under nitrate in C3 plants. Ecology. 93, 355–367.

Bloom, A. J. 2015. Photorespiration and nitrate assimilation: a major intersection between plant carbon and nitrogen. Photosynth Res. 123, 117–128.

Bloom, A.J., Burger, M., Kimball, B.A., Pinter, P.J. 2014. Nitrate assimilation is inhibited by elevated CO2 in field-grown wheat. Nat. Clim. Change. 4, 1758–6798.

Bloom, A.J., Burger, M., Rubio Asensio, J.S., Cousins, A.B. 2010. Carbon dioxide enrichment inhibits nitrate assimilation in wheat and Arabidopsis. Science. 328, 899–903.

Bloom, A.J., Smart, D.R., Nguyen, D.T., Searles, P.S. 2002. Nitrogen assimilation and growth of wheat under elevated carbon dioxide. PNAS. 99, 1730–5.

Bolstad, B.M., Irizarry, R., Astrand, M., Speed, T.P. 2003. A comparison of normalization methods for high density oligonucleotide array data based on variance and bias. Bioinformatics. 19, 185–193.

Boyes, D. C. 2001. Growth stage-based phenotypic analysis of Arabidopsis: a model for high throughput functional genomics in plants. The Plant Cell. 13, 1499–1510.

Bradford, M.M. 1976. A rapid and sensitive method for the quantitation of microgram quantities of protein utilizing the principle of protein-dye binding. Anal. Biochem. 72, 248–54.

Britto, D.T., Kronzucker, H.J. 2002. NH_4^+ toxicity in higher plants: a critical review. J Plant Physiol. 159, 567–584.

Britto, D.T., Kronzucker, H.J. 2005) Nitrogen acquisition, PEP carboxylase, and cellular pH

homeostasis: new views on old paradigms. Plant, Cell and Environ. 28, 1396–1409.

Britto, D.T., Siddiqi, M.Y., Glass, A.D., Kronzucker, H.J. 2001. Futile transmembrane NH_4^+ cycling: a cellular hypothesis to explain ammonium toxicity in plants. PNAS. 98, 4255–4258.

Carlisle, E., Myers, S., Raboy, V., Bloom, A. 2012. The effects of inorganic nitrogen form and CO2 concentration on wheat yield and nutrient accumulation and distribution. Front. Plant Sci. 3, 1–13.

Chaves MM, Flexas J, Pinheiro C. 2009. Photosynthesis under drought and salt stress: regulation mechanisms from whole plant to cell. Ann. Bot. 103, 551–560.

Chen, Z.-H., Wang, Y., Wang, J.-W., Babla, M., Zhao, C., García-Mata, C., Sani, E., Differ, C., Mak, M., Hills, A., Amtmann, A., Blatt, M.R., 2016. Nitrate reductase mutation alters potassium nutrition as well as nitric oxide-mediated control of guard cell ion channels in Arabidopsis. New Phytol. 209, 1456–1469.

Crawford, L.A., Bown, A.W., Breitkreuz, K.E., Guinel, F.C. 1994. The synthesis of [gamma]-aminobutyric acid in response to treatments reducing cytosolic pH. Plant Physiol. 104, 865–871.

Cruz, C., Domínguez-Valdivia, M.D., Aparicio-Tejo, P.M., Lamsfus, C., Bio, A., Martins-Loução, M.A., Moran, J.F. 2011. Intra-specific variation in pea responses to ammonium nutrition leads to different degrees of tolerance. Environ Exp Bot. 70, 233–243.

Du, S., Zhang, R., Zhang, P., Liu, H., Yan, M., Chen, N., Xie, H., Ke, S., 2016. Elevated CO2 - induced production of nitric oxide (NO) by NO synthase differentially affects nitrate reductase activity in Arabidopsis plants under different nitrate supplies. J. Exp. Bot. 67, 893–904.

Epron, D., Godard, D., Cornic, G., Genty, B. 1995 Limitation of net CO_2 assimilation rate by internal resistances to CO2 transfer in the leaves of two tree species (Fagus sylvatica L. & Castanea sativa Mill.). Plant Cell Environ. 18, 43–51

Foyer, C.H., Neukermans, J., Queval, G., Noctor, G., Harbinson, J. 2012. Photosynthetic control of electron transport and the regulation of gene expression. J Exp Bot. 63, 1637–61.

Fukayama, H., Sugino, M., Fukuda, T., Masumoto, C., Taniguchi, Y., Okada, M., Sameshima, R., Hatanaka, T., Misoo, S., Hasegawa, T., Miyao, M., 2011. Gene expression profiling of rice grown in free air CO2 enrichment (FACE) and elevated soil temperature. F. Crop. Res. 121, 195–199.

Gerendás, J., Zhu, Z., Bendixen, R., Ratcliffe, R.G., Sattelmacher, B. 1997. Physiological and

biochemical processes related to ammonium toxicity in higher plants. J. Plant Nutr. 160, 239–251.

Guo, S., Schinner, K., Sattelmacher, B., Hansen, U.-P. 2005. Different apparent CO_2 compensation points in nitrate- and ammonium-grown Phaseolus vulgaris and the relationship to non-photorespiratory CO_2 evolution. Physiol. Plant. 123, 288–301.

Guo, H., Sun, Y., Li, Y., Liu, X., Ren, Q., Zhu-Salzman, K., Ge, F., 2013. Elevated CO2 Modifies N Acquisition of Medicago truncatula by Enhancing N Fixation and Reducing Nitrate Uptake from Soil. PLoS One 8, e81373.

Hachiya, T., Sugiura, D., Kojima, M., Sato, S., Yanagisawa, S., Sakakibara, H., Therashima, I., Noguchi, K. 2014. High CO_2 triggers preferential root growth of Arabidopsis thaliana via two distinct systems under low pH and low N stresses. Plant Cell Physiol. 55, 269–280.

Hachiya, T., Watanabe, C.K., Fujimoto, M., Ishikawa, T., Takahara, K., Kawai-Yamada, M., Uchimiya, H., Uesono, Y., Terashima, I., Noguchi, K., 2014. Nitrate addition alleviates ammonium toxicity without lessening ammonium accumulation, organic acid depletion and inorganic cation depletion in *Arabidopsis thaliana* shoots. Plant Cell Physiol. 53, 577–91.

Harley, P.C., Loreto, F., Di Marco, G., Sharkey, T.D. 1992. Theoretical considerations when estimating the mesophyll conductance to CO_2 flux by analysis of the response of photosynthesis to CO2 . Plant Physiol, 98, 1429–1436

Jauregui, I., Aroca, R., Garnica, M., Zamarreño, Á.M., García-Mina, J.M., Serret, M.D., Parry, M., Irigoyen, J.J., Aranjuelo, I., 2015. Nitrogen assimilation and transpiration: Key processes conditioning responsiveness of wheat to elevated [CO_2] and temperature. Physiol. Plant. 155, 338–354. doi:10.1111/ppl.12345

Jauregui, I., Aparicio-Tejo, P.M., Avila, C., Rueda-López, M., Aranjuelo, I. 2015. Root and shoot performance of Arabidopsis thaliana exposed to elevated CO_2: a physiologic, metabolic and transcriptomic response. J. Plant Physiol. 189, 65-76

Jauregui, I., Aparicio-Tejo, P.M., Avila, C., Cañas, R., Sakalauskiene, S., Aranjuelo, 2016. Root-shoot interactions explain the reduction of leaf mineral content in Arabidopsis plants grown under elevated [CO_2] conditions. Phys. Plant. 158, 65-79.

Keurentjes, J.J.B., Sulpice, R., Gibon, Y., Steinhauser, C., Fu, J., Koornneef, M., Stitt, M., Vreugdenhil, D. 2008. Integrative analyses of genetic variation in enzyme activities of primary carbohydrate metabolism reveal distinct modes of regulation in Arabidopsis thaliana. Genome Biol. 9, R129.

Lawlor, D.W., Tezara,W. 2009. Causes of decreased photosynthetic rate and metabolic capacity in water deficient leaf cells: a critical evaluation of mechanismsandintegration of processes. Ann. Bot. 103, 561–579.

Leakey, A.D.B., Xu, F., Gillespie, K.M., McGrath, J.M., Ainsworth, E.A., Ort, D.R. 2009. Genomic basis for stimulated respiration by plants growing under elevated carbon dioxide. PNAS. 106, 3597–3602.

Lemoine, R., La Camera, S., Atanassova, R., Dédaldéchamp, F., Allario, T., Pourtau, N., Bonnemain, J.-L., Laloi, M., Coutos-Thévenot, P., Maurousset, L., Faucher, M., Girousse, C., Lemonnier, P., Parrilla, J., Durand, M., 2013. Source-to-sink transport of sugar and regulation by environmental factors. Front. Plant Sci. 4, 272.

Li, P., Ainsworth, E.A., Leakey, A.D.B., Ulanov, A., Lozovaya, V., Ort, D.R., Bohnert, H.J. 2008. Arabidopsis transcript and metabolite profiles: ecotype-specific responses to open-air elevated [CO_2]. Plant, Cell Environ. 3*1*, 1673–1687.

Liao, Z., Chen, M., Guo, L., Gong, Y., Tang, F., Sun, X., Tang, K. 2004. Rapid isolation of high-quality total RNA from taxus and ginkgo. Prep. Biochem. Biotechnol. 34, 209–214.

Liu, Y., von Wirén, N., 2017. Ammonium as a signal for physiological and morphological responses in plants. J. Exp. Bot. 63, 3777–3788.

Loladze, I. 2014. Hidden shift of the ionome of plants exposed to elevated CO_2 depletes minerals at the base of human nutrition. *eLIFE*, 1–29. doi.org/10.7554/eLife.02245

Markelz, R.J.C., Lai, L.X., Vosseler, L.N., Leakey, A.D.B. 2013. Transcriptional reprogramming and stimulation of leaf respiration by elevated CO_2 concentration is diminished, but not eliminated, under limiting nitrogen supply. Plant, Cell Environ. 37, 886–898.

Martinoia, E., Maeshima, M., Neuhaus, H.E. 2007. Vacuolar transporters and their essential role in plant metabolism. J. Exp. Bot. 58, 83–102.

Niinemets, Ü., Kull, O. 2001. Sensitivity to photoinhibition of photosynthetic electron transport in a temperate deciduous forest canopy: Photosystem II centre openness, non-radiative energy dissipation and excess irradiance under field conditions. Tree Physiol. 21, 899–914

Niu, Y., Chai, R., Dong, H., Wang, H., Tang, C., Zhang, Y. 2013. Effect of elevated CO_2 on phosphorus nutrition of phosphate-deficient *Arabidopsis thaliana* (L.) Heynh under different nitrogen forms. J. Exp. Bot. 64, 355–367.

Niu, Y., Golam, J.A.,Caixian, T.,Longbiao, G., Jingquan Y., 2016 Physiological and

Transcriptome Responses to Combinations of Elevated CO_2 and Magnesium in Arabidopsis thaliana. PLOS-One. 16, doi.org/10.1371/journal.pone.0149301

Pracharoenwattana, I., Zhou, W., Keech, O., Francisco, P.B., Udomchalothorn, T., Tschoep, H., Stitt, M., Gibon, Y., Smith, S.M. 2010. Arabidopsis has a cytosolic fumarase required for the massive allocation of photosynthate into fumaric acid and for rapid plant growth on high nitrogen. 62, 785–795

Periappuram C, Steinhauer L, Barton DL, Taylor DC, Chatson B., and Zou, J. 2000. The plastidic phosphoglucomutase from Arabidopsis. A reversible enzyme reaction with an important role in metabolic control. Plant Physiol. 122, 1193–1199.

Podgórska, A, Gieczewska, K, Łukawska-Kuźma, K, Rasmusson, AG, Gardeström, P, Szal, B. 2013. Long-term ammonium nutrition of Arabidopsis increases the extrachloroplastic NADPH/$NADP^+$ ratio and mitochondrial reactive oxygen species level in leaves but does not impair photosynthetic capacity. Plant Cell Environ. 36, 2034–2045.

Puppo A, Rigaud, J. 1975. Indole-3-acetic acid catabolism by soybean bacteroids. Physiol. Plant. 35, 223–228.

Raven, J. A. 1986. Biochemical disposal of excess H+ in growing plants? New Phytol. 104, 175–206.

Rubio-Asensio, J.S., Bloom, A.J. 2016. Inorganic nitrogen form: a major player in wheat and Arabidopsis responses to elevated CO_2. J. Exp. Bot. 165, doi.org/10.1093/jxb/ erw465

Rubio-Asensio, J.S., Rachmilevitch, S., Bloom, AJ. 2015. Responses of Arabidopsis and wheat to rising CO_2 depend on nitrogen source and nighttime CO_2 levels. Plant Physiol. 168, 156-63

Runge, M. 1983. Physiological Plant Ecology III. Springer Berlin Heidelberg.

Sarasketa, A., Gonzalez-Moro, M.B., Gonzalez-Murua, C., Marino, D. 2014. Exploring ammonium tolerance in a large panel of *Arabidopsis thaliana* natural accessions. J. Exp. Bot. 65, 6023–6033.

Sharkey, T.D., Bernacchi, C.J., Farquhar, G D., Singsaas, E.L. 2007. Fitting photosynthetic carbon dioxide response curves for C3 leaves. *Plant Cell Environ.* 30, 1035–40.

Smyth, G. K. 2004. Linear models and empirical bayes methods for assessing differential

expression in microarray experiments. Stat. Appl. Genet. Mol. Biol. 3, Article3.

Takatani, N., Ito, T., Kiba, T., Mori, M., Miyamoto, T., Maeda, S.-I., Omata, T. 2014. Effects of high CO_2 on growth and metabolism of arabidopsis seedlings during growth with a constantly limited supply of nitrogen. Plant Cell Physiol. 55, 281–292.

Taub, D.R., Miller, B., Allen, H. 2008. Effects of elevated CO_2 on the protein concentration of food crops: a meta-analysis. Global Change Biol. 14, 565–575.

Thimm, O., Bläsing, O., Gibon, Y., Nagel, A., Meyer, S., Krüger, P., Selbig, J., Müller, L.A., Rhee, S.Y., Stitt, M., 2004. mapman: a user-driven tool to display genomics data sets onto diagrams of metabolic pathways and other biological processes. Plant J. 37, 914–939.

Unkles, S.E., Wang, R., Wang, Y., Glass, A.D.M., Crawford, N.M., Kinghorn, J.R., 2004.

Nitrate reductase activity is required for nitrate uptake into fungal but not plant cells. J. Biol.

Chem. 279, 28182–6.

Wang, R., Tischner, R., Gutierrez, R.A.,Hoffman, M., Xing, X., Wang, R., Tischner, R., Gutie, R. A., Chen, M., Coruzzi, G., Crawford, N.M. 2004. Genomic analysis of the nitrate response using a nitrate reductase-null mutant of Arabidopsis. Plant Physiol. 136, 2512–2522.

Watanabe, C.K., Sato, S., Yanagisawa, S., Uesono, Y., Terashima, I., Noguchi, K. 2014. Effects of elevated CO_2 on levels of primary metabolites and transcripts of genes encoding respiratory enzymes and their diurnal patterns in Arabidopsis thaliana: Possible Relationships with Respiratory Rates. Plant Cell Physiol. 55, 341–357.

Wilkinson, J.Q., Crawford, N.M. 1993. Identification and characterization of a chlorate-resistant mutant of Arabidopsis thaliana with mutations in both nitrate reductase structural genes NIA1 and NIA2. Mol. Gen. Genet. 239, 289–297.

Figure 1. Effect of elevated [CO_2] (800 *versus* 400 ppm) applied to *Arabidopsis thaliana* wild type plants (col. 0) and the NR mutant genotype on shoot (A-A´) and root (B-B´) plant weight (dry matter) basis. Data were analyzed using a one-factor analysis of variance (ANOVA). The different letters above the columns indicate significant differences ($P < 0.05$) between treatments as determined by the Tukey b test. The symbols * or # indicate the higher value for each genotype. Values represent the means of 12 replicates ± SE.

Figure 2. Effect of elevated [CO_2] (800 *versus* 400 ppm) applied to *Arabidopsis thaliana* wild type plants (col. 0) and the NR mutant genotype on net photosynthesis, An, (A-A´); the maximum rate of Rubisco carboxylase activity, Vc_{max} (B-B´); the maximum electron transport rate contributing to RuBP regeneration, J_{max}, (C-C´); leaf dark respiration, Rd (D-D´); and intercellular [CO_2], Ci. Data were analyzed using a one-factor analysis of variance (ANOVA). The different letters above the columns indicate significant differences ($P < 0.05$) between treatments as determined by the Tukey b test. The symbols * or # indicate the higher value for each genotype. Values represent the means of 6 replicates ± SE.

Figure 3. Effect of elevated [CO_2] (800 *versus* 400 ppm) applied to *Arabidopsis thaliana* wild type plants (col. 0) and the NR mutant genotype on electron transport rate, Je(PSII), (A-A´) in µmo $e^{-}m^{-2}$ s^{-1}; electron flux for photosynthetic carbon reduction, Je(PCR) in µmo $e^{-}m^{-2}$ s^{-1}; (B-B´), electron flux for photosynthetic for photorespiration, Je(PCO) (C-C´) in µmol $e^{-}m^{-2}$ s^{-1}; the ETRc/ ETRo ratio, (D-D´); and the relative quantum yield of PSII at the steady state, ΦPSII, (E, E´). Data were analyzed using a one-factor analysis of variance (ANOVA). The different letters above the columns indicate significant differences ($P < 0.05$) between treatments as determined by the Tukey b test. The symbols * or # indicate the higher value for each genotype. Values represent the means of 6 replicates ± SE

Figure 4. Effect of elevated [CO_2] (800 *versus* 400 ppm) applied to *Arabidopsis thaliana* wild type plants (col. 0) and the NR mutant genotype on carbohydrate content in the leaves (A-A´; C-C´) and roots (B-B´; D-D´): sucrose, glucose, fructose and starch. Data were analyzed using a one-factor analysis of variance (ANOVA). The different letters above the columns indicate significant differences ($P < 0.05$) between treatments as determined by the Tukey b test. The symbols * or # indicate the higher value for each genotype. Values represent the means of 4 replicates ± SE.

Figure 5. Heat map of transcripts in selected gene families of leaves of the *Arabidopsis thaliana* NR mutant genotype exposed to [CO_2] (800 versus 400 ppm). Significant $\log_2$ expression changes in elevated [CO_2] (red color) versus ambient (blue color) are indicated.

Figure 1

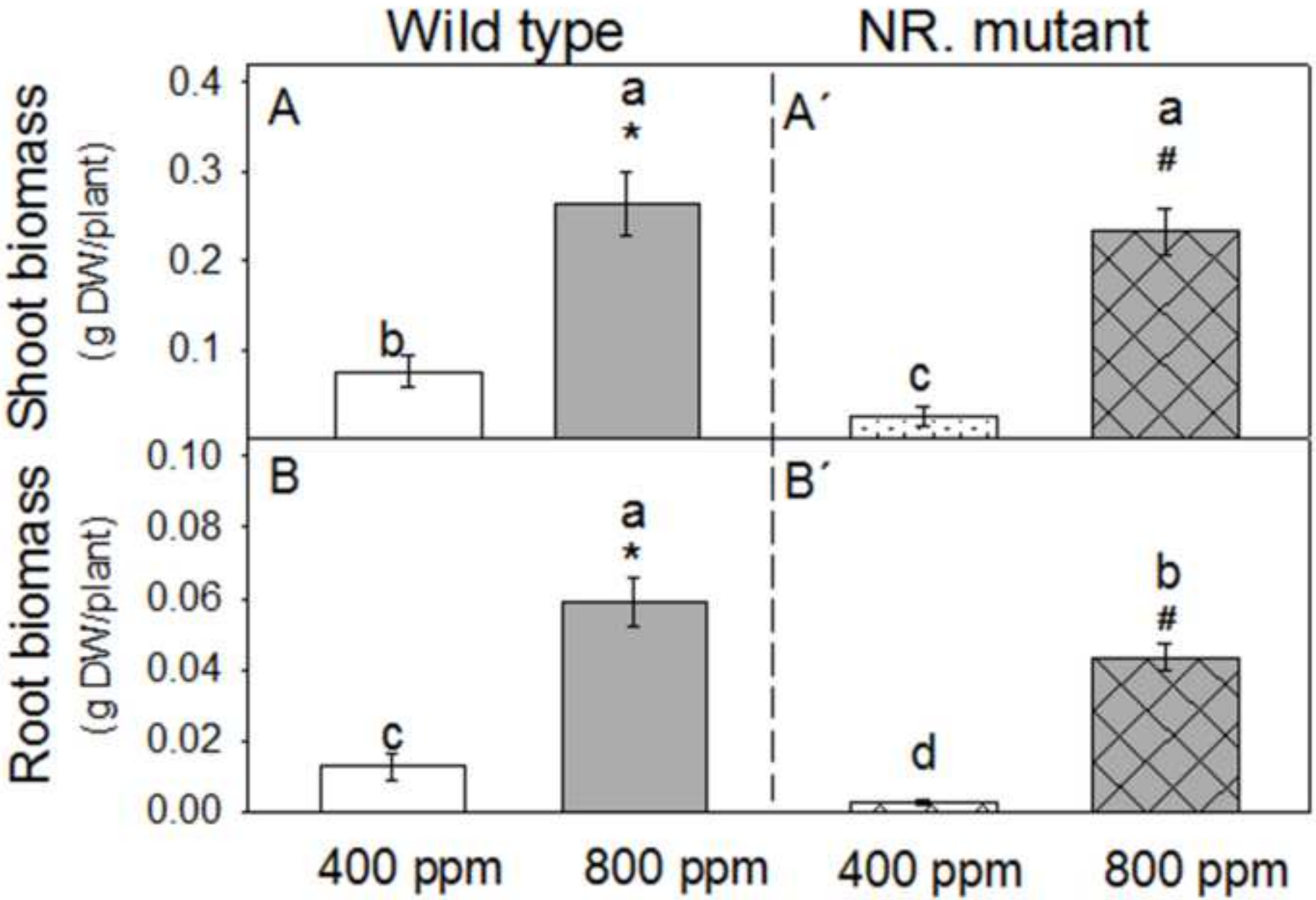
Wild type
NR. mutant
Shoot biomass
(g DW/plant)
Root biomass
(g DW/plant)
A
A´
B
B´
a
b
c
d
*
#
0.4
0.3
0.2
0.1
0.10
0.08
0.06
0.04
0.02
0.00
400 ppm
800 ppm
400 ppm
800 ppm

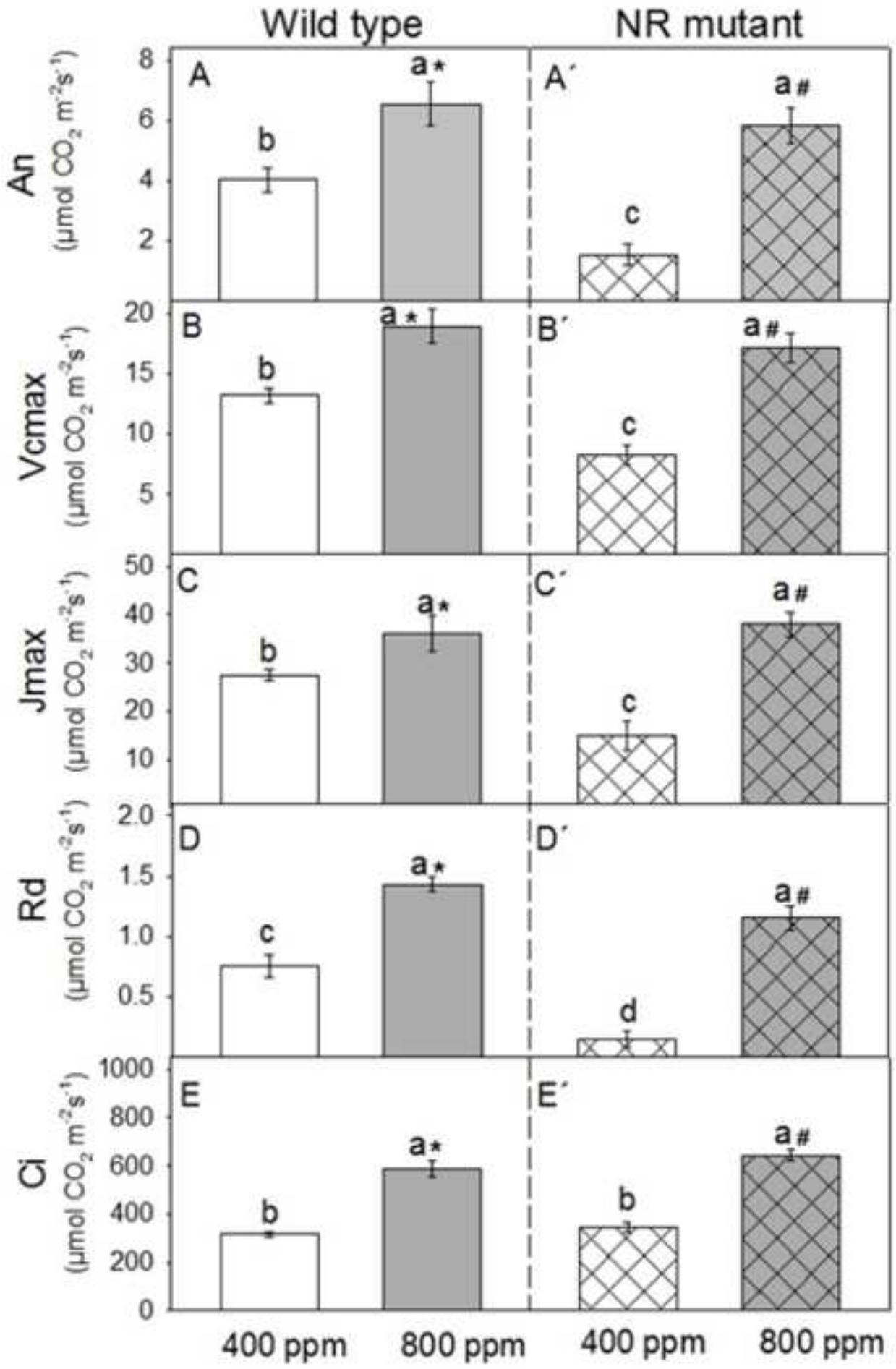

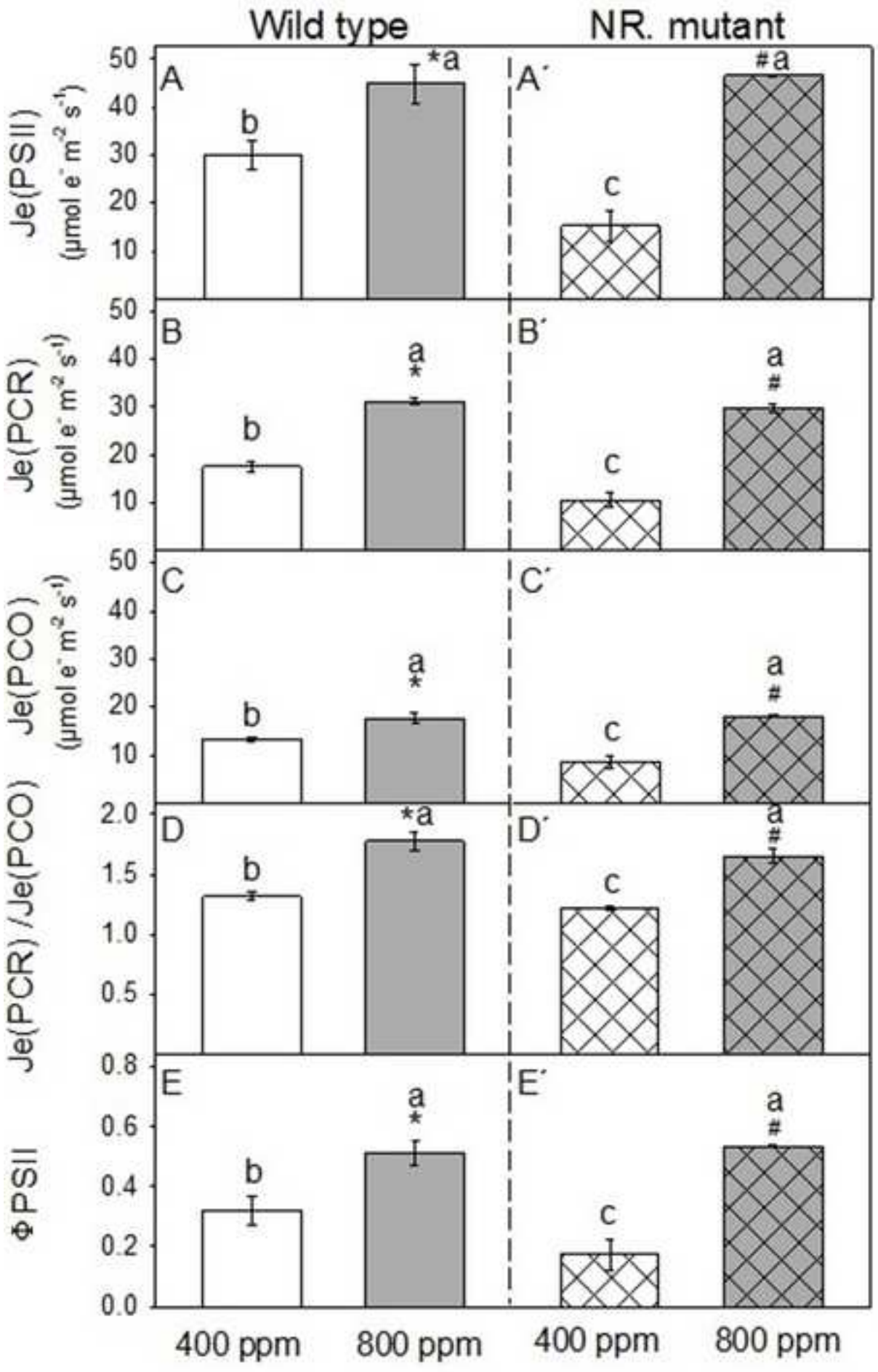

Figure 4

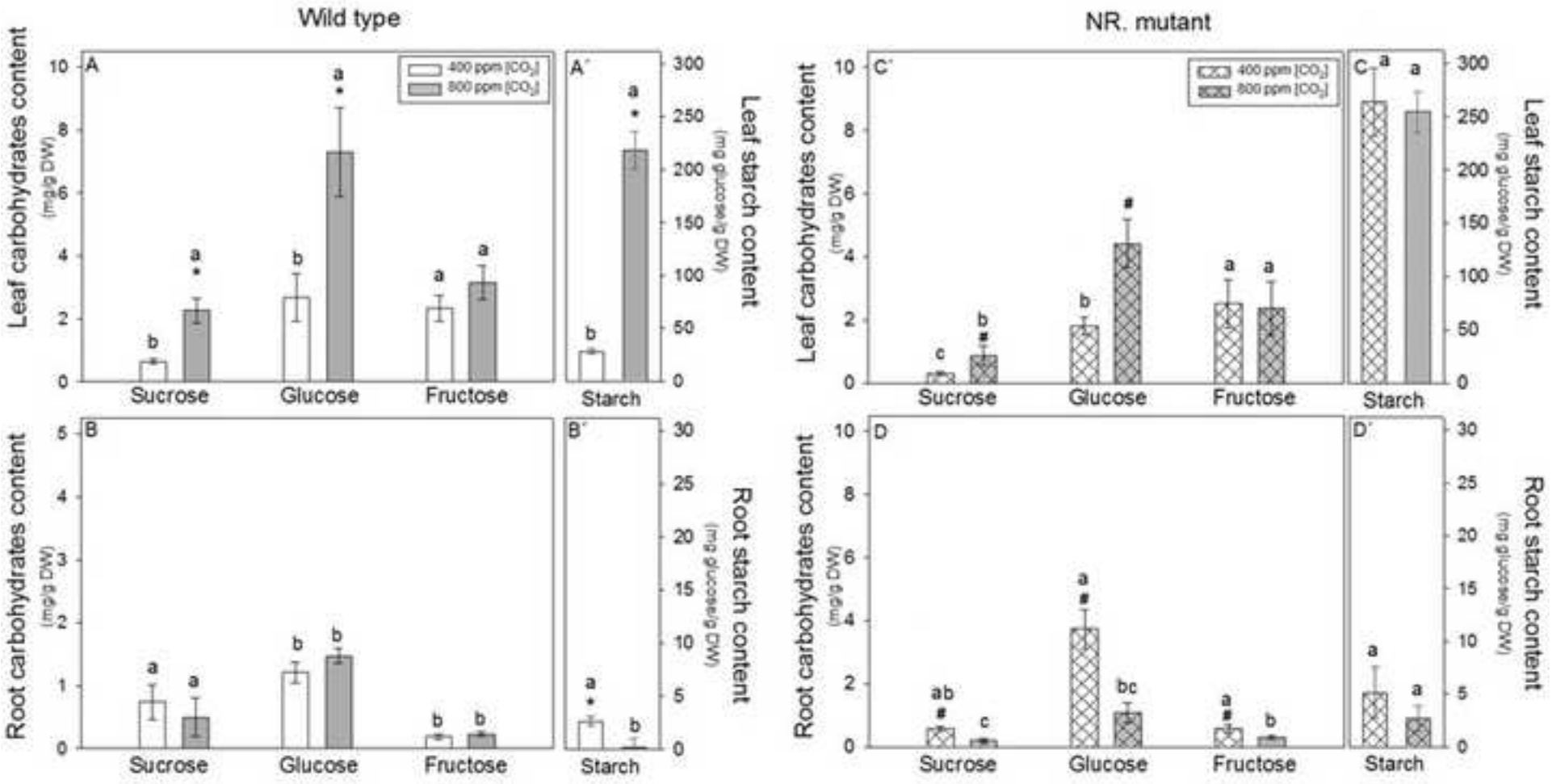
Wild type
NR. mutant
400 ppm [CO2]
800 ppm [CO2]
Leaf carbohydrates content
(mg/g DW)
Leaf starch content
(mg glucose/g DW)
Root carbohydrates content
(mg/g DW)
Root starch content
(mg glucose/g DW)
Sucrose
Glucose
Fructose
Starch
A
A'
B
B'
C
C'
D
D'

Figure 5

Bin name	Tair	Gene name
light harvest/photosynthesis	at2g30790	Photosystem II subunit P-2
	at4g18360	Glycolate oxidase 3
	at4g32590	at4g32590
	at5g44520	at5g44520
	at1g73110	at1g73110
	at4g20130	Plastic transcriptionally active 14
	at5g36120	cofactor assembly, complex C (B6F)
	at1g60950	Ferredoxin-2, chloroplastic
	at3g04790	Probable ribose-5-phosphate isomerase 3
	at2g35370	Glycine decarboxylase complex H
	at1g20020	Ferredoxin-NADP(+)-Oxidoreductase 2,
	at1g15140	FAD/NAD(P)-binding oxidoreductase;
	at1g05385	Photosystem II 11 kDa protein-related
	at2g26500	cytochrome b6f complex subunit (petM)
	at3g55800	Sedoheptulose-1,7-bisphosphatase
	at3g01440	PsbQ-like protein 2, chloroplastic
	at1g14150	PsbQ-like protein 1, chloroplastic
	at1g70760	Chlororespiratory reduction 23,
	at1g44575	Photosystem II 22 kDa protein
	at5g51545	Protein low PSII accumulation 2
	at1g14030	Fructose-bisphosphate aldolase
	at2g39470	PsbP-like protein 2 (PPL2)
	at1g11860	Glycine cleavage T-protein family
	at4g28660	Photosystem II reaction center PSB28
	at3g55330	PsbP-like protein 1, chloroplastic
	at1g55490	Chaperonin 60 beta

Bin name	Tair	Gene name
light harv...	at3g56650	PSBP-Domain protein 6
	at2g40100	Lhcb4.3, light harvesting complex of photosystem II
	at5g11450	PSBP Domain protein 5
Glycolisys	at2g22480	Phosphofructokinase 5
	at4g26270	Phosphofructokinase 3
	at1g70820	phosphoglucomutase, putative
PPP	at1g13700	6-Phosphogluconalactonase 1,
	at5g13420	Aldolase-type TIM barrel family protein
	at1g24280	Glucose-6-phosphate 1-dehydrogenase 3
Tricarboxylic acid	at2g19900	NADP-Malic enzyme 1
	at5g65750	2-oxoglutarate dehydrogenase, E1 component
	at2g05710	Aconitase 3
	at5g50950	fumarate hydratase 2
glyoxylate cycle	at2g42790	citrate synthase 3
Redox	at5g39950	Thioredoxin H2
	at1g59730	Thioredoxin H7
	at5g42980	Thioredoxin H3
	at1g45145	Thioredoxin H5
	at4g08390	L-ascorbate peroxidase S
	at5g20140	Glutaredoxin-C3
	at5g23310	Superoxide dismutase [Fe] 3, chloroplastic
	at2g20270	Monothiol glutaredoxin-S12, chloroplastic
	at4g09010	ascorbate peroxidase 4
	at4g31870	Putative glutathione peroxidase 7, chloroplastic
	at5g51100	Superoxide dismutase [Fe] 2, chloroplastic
	at3g26060	Peroxiredoxin Q, chloroplastic

Table 1. Effect of elevated [CO_2] (800 *versus* 400 ppm) applied to *Arabidopsis thaliana* wild type plants (col. 0) and the NR mutant genotype on leaf N concentration (g/100g), the leaf C/N ratio, leaf and root total soluble protein (TSP mg prot g DM^{-1}), and leaf and root ammonium concentrations (NH_4^+, mg g^{-1} DM). Data were analyzed using a one-factor analysis of variance (ANOVA). The different letters above the columns indicate significant differences ($P < 0.05$) between treatments, determined with the Tukey b test. The symbols in bold indicate higher values for each genotype. Values represent the means of 4 replicates ± SE**.**

		Leaf N	**Leaf C/N ratio**	**Leaf TSP**	**Root TSP**	**Leaf NH_4^+ content**	**Root NH_4^+ content**	**Leaf NH_4^+ content**	**Leaf NO_3^- content**	**Root NO_3^- content**
Wild type	**400 ppm**	6.97 ± 0.14 b	5.13 ± 0.06 a	**134.6** ± 9.4 b	73.4± 3.4 ab	**5.04 ± 0.75 b**	33.5± 1.1 b	**5.04 ± 0.75 b**	**44.4 ± 5.6 c**	152 ± 19 ab
	800 ppm	6.88 ± 0.075 b	5.02 ± 0.03a	124.6 ± 7.0 bc	67.3 ± 6.7 b	1.86 ± 0.25 c	32.1 ± 0.4 b	1.86 ± 0.25 c	30.3 ± 4.4 d	136 ± 18 b
NR mutant	**400 ppm**	**7.50 ± 0.17 a**	4.13 ± 0.20 b	**171.9 ± 17.6 a**	89.9 ± 7.6 a	**15.6 ± 0.53 a**	24.45 ± 2.8 c	**15.6 ± 0.53 a**	**65.9 ± 5.7 a**	**170 ± 31 a**
	800 ppm	6.85 ± 0.19 b	4.78 ± 0.19 a	142.4 ± 9.2 b	76.1 ± 10.4 ab	5.2 ± 0.79 b	**40.4 ± 8.8 a**	5.2 ± 0.79 b	54.7 ± 1.8 b	134 ± 6 b

Table 2. Global functional enrichment analysis for significant genes of *Arabidopsis thaliana* wild type plants (col. 0) and the NR mutant genotype exposed to [CO_2] (800 versus 400 ppm). The functional enrichment analysis was based on the functional Mapman categories and performed using the LIMMA test. The data set included the total, the upregulated and the downregulated genes at the 800 ppm [CO_2] treatment. Values represent 3 replicates per treatment and tissue, and significant differences in gene expression had a *Q value* ≤ 0.05 and $\log_2$ fold change ≥ 0.5.

	Leaf tissue						**Root tissue**					
	Wild type			NR mutant			Wild type			NR mutant		
	Total	**down**	**up**	**Total**	down	up	**Total**	down	up	**Total**	down	up
Photosynthesis	**1**	0	1	**29**	27	2	**3**	3	0	**30**	4	26
Major CHO metabolism	**1**	0	1	**15**	3	12	**1**	0	1	**3**	1	2
Minor CHO metabolism	**1**	1	0	**19**	9	10	**8**	2	6	**17**	6	11

Glycolysis	**0**	0	0	**6**	2	4	**2**	0	2	**7**	7	0
Fermentation	**0**	0	0	**2**	0	2	**0**	0	0	**1**	0	1
Gluconeogenesis/ glyoxylate cycle	**0**	0	0	**1**	0	1	**0**	0	0	**0**	0	0
Oxidative pentose phosphate cycle	**0**	0	0	**6**	3	3	**0**	0	0	**8**	7	1
Tricarboxylic acid cycle	**1**	1	0	**7**	2	5	**0**	0	0	**4**	2	2
Electron transport/ ATP	**1**	0	1	**9**	5	4	**3**	3	0	**10**	8	2
Cell wall	**4**	0	4	**33**	16	17	**23**	19	4	**36**	27	9
Lipid metabolism	**5**	1	4	**46**	20	26	**20**	12	8	**32**	15	17
N-metabolism	**0**	0	0	**2**	0	2	**1**	1	0	**4**	3	1
Amino acid metabolism	**4**	0	4	**29**	19	10	**6**	3	3	**24**	10	14
S-assimilation	**0**	0	0	**2**	1	1	**3**	3	0	**2**	1	1
Metal handling	**2**	0	2	**11**	4	7	**6**	4	2	**13**	6	7
Secondary metabolism	**8**	1	7	**51**	18	33	**16**	7	9	**37**	29	8
Hormone metabolism	**10**	5	5	**33**	10	23	**22**	16	6	**36**	26	10
Co-factor and vitamin metabolism	**1**	0	1	**7**	4	3	**4**	0	4	**5**	2	3
Tetrapyrrole synthesis	**1**	0	1	**15**	14	1	**2**	0	2	**4**	1	3
Stress	**17**	2	15	**104**	18	86	**43**	20	23	**65**	27	38
Redox	**0**	0	0	**26**	16	10	**7**	1	6	**15**	6	9
Polyamine metabolism	**0**	0	0	**2**	1	1	**1**	1	0	**0**	0	0
Nucleotide metabolism	**0**	0	0	**22**	11	11	**5**	4	1	**8**	4	4
Biodegradation of xenobiotics	**0**	0	0	**3**	0	3	**3**	1	2	**3**	1	2
C1-metabolism	**0**	0	0	**3**	0	3	**2**	1	1	**2**	2	0
Miscellaneous	**19**	3	16	**144**	48	96	**61**	28	33	**95**	46	49
RNA	**19**	5	14	**164**	92	72	**93**	49	44	**148**	68	80
DNA	**1**	0	1	**25**	19	6	**7**	3	4	**12**	7	5
Protein	**20**	8	12	**284**	151	133	**108**	41	67	**156**	64	92
Signaling	**23**	5	18	**106**	26	80	**37**	16	21	**56**	33	23
Cell	**5**	0	5	**51**	28	23	**23**	12	11	**38**	20	18
microRNA	**0**	0	0	**8**	2	6	**1**	0	1	**11**	9	2
Development	**4**	2	2	**64**	29	35	**32**	19	13	**47**	19	28
Transport	**6**	1	5	**92**	19	73	**44**	19	25	**51**	31	20
Unknown	**58**	19	39	**526**	299	227	**269**	180	89	**399**	232	167
Total	**212**	54	158	**1947**	916	1031	**856**	468	388	**1379**	724	655